Modal analysis of isotropic beams in peridynamics

Andris Freimanis[1,*], Ainārs Paeglītis[1]

[1]Riga Technical university, Institute of Transportation Engineering, Azenes iela 6a, Riga, Latvia, LV-1048

E-mail: *andris.freimanis_1@edu.rtu.lv

Abstract. Modal analysis in continuum mechanics is widely used in damage detection, quality control and to validate numerical simulations. Peridynamics is a reformulation of continuum mechanics that allow discontinuities, such as cracks and voids, to arise and propagate without any special techniques, however, modal analysis in peridynamics has not been explored in detail. In this study we simulate the modal response of an aluminium plate with clamped-free boundary conditions in peridynamics, and compare results to a FE simulation and an experimental modal test. The natural frequencies from peridynamics agree better with the experimental results than frequencies from finite-elements for all modes except mode 1. Differences between peridynamic and experimental results ranged (in magnitude) from 0.13% to 10.38%, and between peridynamic and finite-element results from 0.23% to 9.72%. All mode shapes calculated in peridynamics corresponded to those from finite-elements and experimental measurements.

1. Introduction

Natural frequencies and mode shapes, together called modes, are determined by the material properties i.e. mass, damping, stiffness, and object's boundary conditions. If either of these properties change, then the modes of an object will change. This is used to detect damage in structures, control manufacturing quality, validate simulations etc. [1]–[4].

Peridynamics (PD) is a reformulation of classical continuum mechanics (CM) that allows discontinuities, such as cracks in damaged structures, to be modelled without any special techniques. PD was first introduced in the bond-based form [5] and later extended to state-based form [6], in this article we only use the state-based PD. Modal analysis in PD has been explored in [7], where a good agreement between a two-dimensional PD simulation, classical mechanics solution, and finite-element (FE) solution was found. In this study we compare the results from PD modal analysis to FE and experimental results.

Continuum mechanics theory uses partial differential equations to represent strain and stress between particles. Since partial derivatives are undefined along discontinuities, cracks can't be modeled without the additional assumptions of fracture mechanics. PD is a non-local extension of CM, that uses integral equations and deformation to describe relations between particles, therefore relations remain valid in the presence of discontinuities. Furthermore, elastic PD model reproduces CM model as the non-local interaction distance goes to zero, if the motion, constitutive model and non-homogeneities are sufficiently smooth [8]. A PD body consists of an infinite number of particles, each associated with some volume V_i and identified by its a coordinate $\boldsymbol{x_i}$. A particle $\boldsymbol{x_i}$ interacts through bonds $\langle \boldsymbol{x_i} - \boldsymbol{x_j} \rangle$ with a family of particles $H_{\boldsymbol{x_i}}$, the interaction range is described by the horizon δ, and all interactions vanish beyond the horizon. In three dimensions, this means that a particle $\boldsymbol{x_i}$ interacts

with all particles within a sphere with a radius $\delta > 0$ around itself. The particle $\boldsymbol{x_i}$ is influenced by the collective deformation of all particles in its family $H_{\boldsymbol{x_i}}$. This interaction results in the force density vector $\boldsymbol{t_{ij}}$ acting at particle $\boldsymbol{x_i}$. Similarly, a particle $\boldsymbol{x_j}$ is influenced by the collective deformation of its family $H_{\boldsymbol{x_j}}$ and the force density vector acting at $\boldsymbol{x_j}$ is $\boldsymbol{t_{ji}}$, this vector can be viewed as the force exerted by the particle $\boldsymbol{x_i}$ on the particle $\boldsymbol{x_j}$. Force density vectors $\boldsymbol{t_{ij}}$ are stored in an infinite-dimensional array, called the force vector state, $\boldsymbol{T}$. When an object undergoes displacement $\boldsymbol{u_i}$, the position vector $\boldsymbol{y_i}$ describes a particle's position in the deformed configuration and the relative position vectors in the deformed configuration $\boldsymbol{y_i} - \boldsymbol{y_j}$ are stored in an array called the deformation vector state, $\boldsymbol{Y}$. Since force vector state $\boldsymbol{T}(\boldsymbol{x_i}, t)$ depends on the relative deformation of $H_{\boldsymbol{x_i}}$, it can also be written as $\boldsymbol{T}(\boldsymbol{x_i}, t) = \boldsymbol{T}(\boldsymbol{Y}(\boldsymbol{x_i}, t))$, where t – force scalar state. The peridynamic equation of motion is

$$\rho(\boldsymbol{x_i})\ddot{\boldsymbol{u}}(\boldsymbol{x_i}) = \int_{H_i} (\boldsymbol{T}(\boldsymbol{x_i}, t)\langle \boldsymbol{x_j} - \boldsymbol{x_i}\rangle - \boldsymbol{T}(\boldsymbol{x_j}, t)\,\langle \boldsymbol{x_i} - \boldsymbol{x_j}\rangle) dH_i + b(\boldsymbol{x_i}, t)$$

, where ρ – density, $\ddot{\boldsymbol{u}}$ – acceleration, and b – external force density. Cracks in a body are introduced by breaking bonds when some criterion is reached. The simplest damage model is the critical stretch i.e. a bond is broken when its stretched past some critical value. A very short description of peridynamics is given here, so for further information readers are referred to [9]–[11].

Modal analysis is solved by solving the eigenvalue problem that arises from the equation of motion of some object. In matrix form this equation is:

$$\boldsymbol{M}\ddot{\boldsymbol{u}} + \boldsymbol{C}\dot{\boldsymbol{u}} + \boldsymbol{K}\boldsymbol{u} = \boldsymbol{f},$$

where $\boldsymbol{f}$ – force vector, $\boldsymbol{M}$ – mass matrix, $\boldsymbol{C}$ – damping matrix, $\boldsymbol{K}$ – stiffness matrix, $\boldsymbol{u}$ – displacement vector. We consider undamped free vibrations, so the $\boldsymbol{C}\dot{\boldsymbol{u}}$ term vanishes and force vector $\boldsymbol{f}$ is equal to zero, and the equation of motion is reduced to:

$$\boldsymbol{M}\ddot{\boldsymbol{u}}(t) + \boldsymbol{K}\boldsymbol{u}(t) = 0$$

This equation is solved as generalized eigenvalue problem:

$$\boldsymbol{K}\boldsymbol{x} = \lambda \boldsymbol{M}\boldsymbol{x},$$

where $\boldsymbol{x}$ – eigenvectors, λ – eigenvalues. To solve the generalized eigenvalue problem a shift-inverse transformation is used. The original problem is shifted closer to some value σ and inverted so that the smallest eigenvalues of the original problem becomes the smallest eigenvalues of the transformed problem:

$$\boldsymbol{H}\boldsymbol{x} = \mu \boldsymbol{x}$$

where

$$\boldsymbol{H} = \frac{\boldsymbol{M}}{\boldsymbol{K} - \sigma \boldsymbol{M}} \quad \text{and} \quad \mu = \frac{1}{\lambda - \sigma}.$$

Each eigenvalue λ_i corresponds to one natural frequency f_i, and eigenvector $\boldsymbol{x_i}$ corresponds to the mode shape of f_i. Natural frequencies f_i are related to eigenvalues λ_i through:

$$f_i = \frac{\sqrt{\lambda_i}}{2\pi}.$$

For further discussion about structural dynamics see [12], and for eigenvalue problems see [13].

2. Modal analysis

In this study, we compare natural frequencies and mode shapes from PD simulation with the results from FE and experimental modal analysis. A rectangular aluminium plate clamped at one end and free at the other with side lengths of 0.25m×0.05m×0.002m was used as a benchmark, modal test setup is showed in Figure 1. A piezo-electric element located at the end of the beam induced vibrations, and two-dimensional (2D) Polytec PSV-400 laser vibrometer measured the speed of 115 nodes on the plate. Since 2D vibrometer can't measure out-of-plane and longitudinal nodal speed, we could only extract in-plane bending and torsional modes.

Modal analysis requires stiffness and mass matrices. Peridigm [14] with added custom code was used to create them. Then a Matlab script with Block-Lanczos algorithm [15], [16] calculated natural frequencies and mode shapes. In PD plate was modelled using meshfree approach [17], particle size was 0.0005m and the peridynamic horizon was set to 0.00075. Displacement in all degrees of freedom was fixed for one plane of particles at one end of the plate, creating clamped – free boundary conditions. Material response was modelled using position aware linear solid (PALS) material model [18]. Modulus of elasticity was set to 62.00GPa, shear modulus to 21.83GPa, and density to 2700kg/m^3.

FE analysis was done in Ansys FE software. The plate was simulated using linear elastic material model with the same material properties as in PD analysis. It was meshed with cubic SOLID185 elements with an edge length of 0.0005m. Displacements were fixed in all degrees of freedom for all nodes on one end plane of the plate, creating clamped-free boundary conditions.

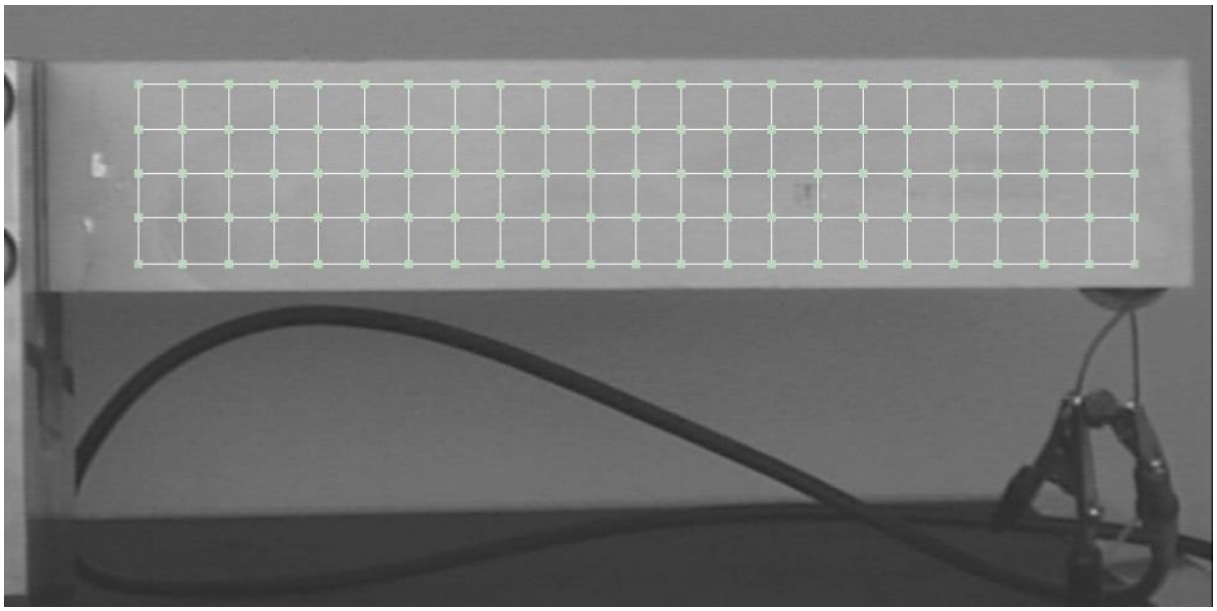

Figure 1. Modal test setup.

3. Results and discussion

The first eight modes were determined in PD simulation, FE simulation and experimentally using a laser vibrometer. Their natural frequencies are showed in Table 1. Natural frequency for Mode 5 couldn't be determined experimentally, because it was an out-of-plane bending mode and 2D vibrometer can't measure in the out-of-plane direction. Percent differences between PD, FE solutions, and experimental natural frequencies are showed in Figure 2. Difference between the experimental results (ER) and PD results in absolute values ranged from 0.13% (mode 7) to 10.38% (mode 1), and between ER and FE results from 1.66% (mode 3) to 13.02% (mode 2). PD results agreed better with ER than FE results in all modes except for mode 1. Natural frequencies in torsional modes (modes 3,

6, 8) computed using both PD and FE analysis were closer to ER than frequencies in bending modes. Possibly the value of shear modulus used in simulations were closer to it's real value, than the value of modulus of elasticity in simulations to the real modulus of elasticity.

We expected better agreement between FE and PD results, because peridynamics converge to the classical theory as the horizon shrinks, and if the deformation field is sufficiently smooth [8]. The differences in absolute values ranged from 0.23% to 9.72%. However, if split by mode type, it can be seen that natural frequencies of in-plane bending modes agreed the worst with differences ranging from 9.05% (mode 7) to 9.72% (mode 2), next were torsional modes for which differences ranged from 3.18% (mode 3) to 3.70% (mode 8), and the best agreement, difference of 0.23%, was between the results of the out-of-plane bending mode (mode 5). A mesh with four particles in plate's height was used, maybe a better agreement can be achieved with a finer mesh, but mesh convergence wasn't studied here.

Table 1. Natural frequencies of the first eight modes computed using PD, FE analysis, and determined experimentally, and percent difference between PD, FE solutions and ER, and between PD and FE results.

Mode	Experimental result (ER)	Peridynamics		Finite-elements		Difference between FE and PD reuslts
		Natrual frequency	Difference from ER	Natrual frequency	Difference from ER	
1	25.63	22.96	10.38%	25.42	0.82%	9.64%
2	140.63	143.48	-2.03%	158.93	-13.02%	9.72%
3	233.75	230.06	1.58%	237.63	-1.66%	3.18%
4	402.50	403.91	-0.35%	446.08	-10.83%	9.45%
5	-	603.90	-	602.49	-	-0.23%
6	713.13	704.37	1.23%	728.95	-2.22%	3.37%
7	797.50	798.50	-0.13%	877.93	-10.09%	9.05%
8	1238.75	1219.44	1.56%	1266.30	-2.22%	3.70%

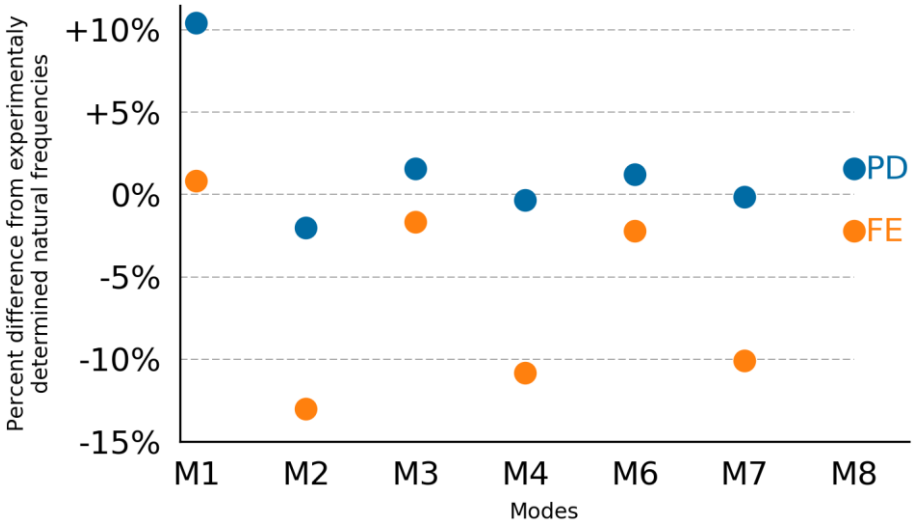

Figure 2. Percent difference between natural frequencies determined experimentally and simulated in peridynamics and finite-elements.

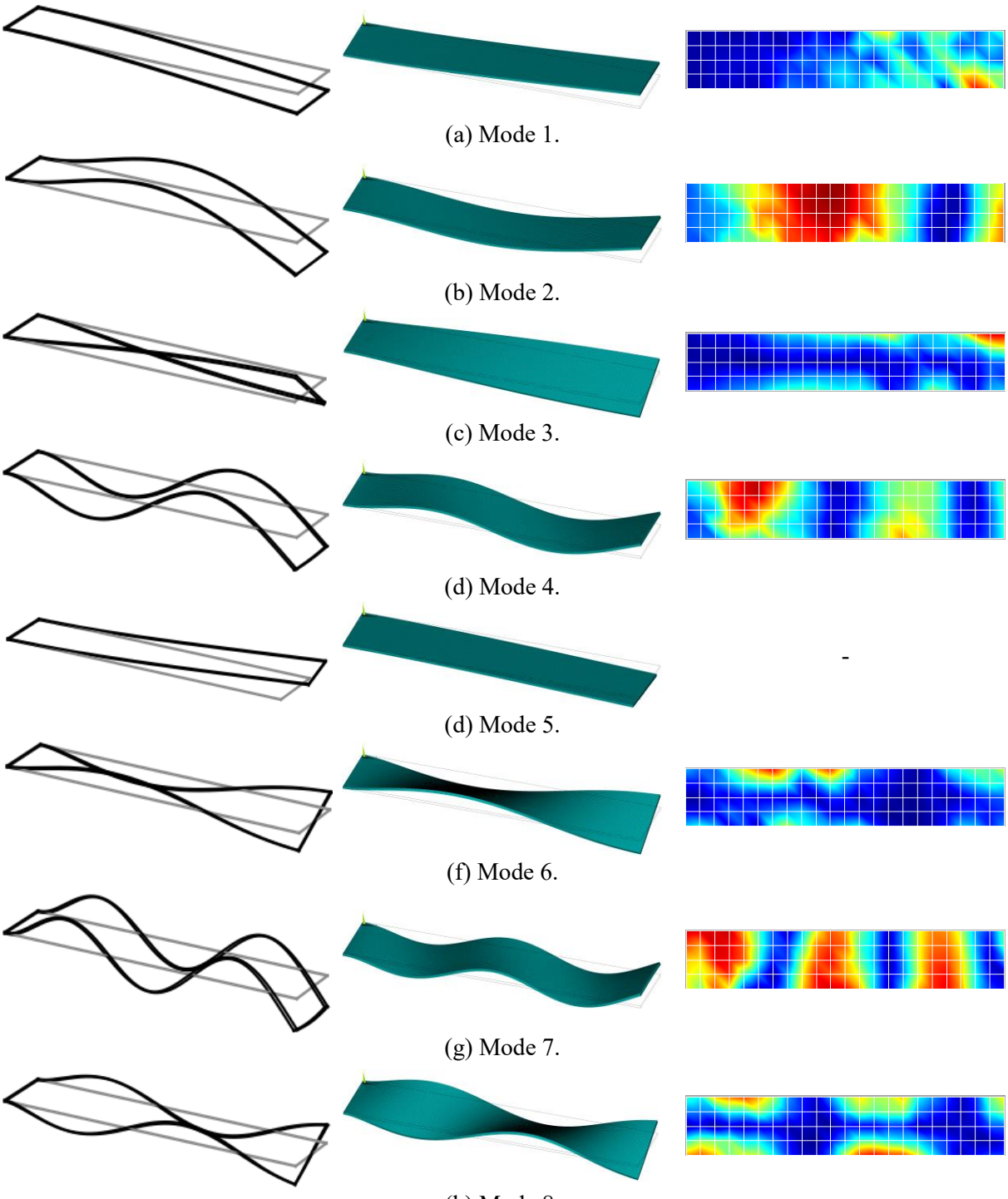

(a) Mode 1.

(b) Mode 2.

(c) Mode 3.

(d) Mode 4.

(d) Mode 5.

(f) Mode 6.

(g) Mode 7.

(h) Mode 8.

Figure 3. Modes shapes from PD simulation (left), FE simulation (center), laser vibrometer (right).

Figure 3 shows mode shapes of the first eight modes from PD, FE analysis and modal test. Mode shapes calculated using PD or FE analysis are showed in three dimensions. Experimentally measured modes are showed as heatmaps with displacements in absolute values, so colors range from blue (values closer to zero) to red (values further from zero). Modes 1 and 2 in all cases are the first two in-plane bending modes, mode 3 is the first torsional mode, and mode 4 is the third in-plane bending mode. Mode 5 is the first out-of-plane bending mode. 2D vibrometer didn't detect it, because it can't

measure in the out-of-plane direction. Modes 6, 7, and 8 are the second torsional mode, the fourth in-plane bending mode, and the third torsional mode respectively. All modes from PD and FE simulations correspond to each other and to those measured experimentally.

4. Conclusions

In this study we did a modal analysis of an aluminium plate, and compared the results to results from finite-element simulation and modal test. Peridynamics showed better agreement with experimental results, than finite-element analysis in all modes except mode 1. We expected peridynamic results to have a better agreement with finite-element results, because peridynamics converge to classical mechanics theory when the horizon shrinks. However, better agreement might be achieved with finer mesh. Mode shapes from peridynamic simulation corresponded to those from finite-element simulation and modal test.

Acknowledgments

This study was partially funded by the Riga Technical University under the project 34-24000-DOK.BIF/16.

The research leading to these results has received the funding from Latvia State Research Programme under grant agreement "Innovative materials and smart technologies for environmental safety, IMATEH".

References

[1] G.-R. Gillich and Z.-I. Praisach, "Modal identification and damage detection in beam-like structures using the power spectrum and time–frequency analysis," *Signal Processing*, vol. 96, pp. 29–44, 2014.

[2] M. Dilena and A. Morassi, "Dynamic testing of a damaged bridge," *Mech. Syst. Signal Process.*, vol. 25, no. 5, pp. 1485–1507, 2011.

[3] V. Quaranta, I. Dimino, M. D'Ischia, G. Davi, and G. Daví, "Modal Analysis on a Schematic Aerospace Structure : FEM Simulation and Experimental Updating," *Conf. Expo. Struct. Dyn.*, 2005.

[4] S. W. Doebling, C. R. Farrar, M. B. Prime, and D. W. Shevitz, "Damage identification and health monitoring of structural and mechanical systems from changes in their vibration characteristics: A literature review," Los Alamos, NM, May 1996.

[5] S. A. Silling, "Reformulation of elasticity theory for discontinuities and long-range forces," *J. Mech. Phys. Solids*, vol. 48, no. 1, pp. 175–209, 2000.

[6] S. A. Silling, M. Epton, O. Weckner, J. Xu, and E. Askari, "Peridynamic states and constitutive modeling," *J. Elast.*, vol. 88, no. 2, pp. 151–184, 2007.

[7] D. J. Littlewood, K. Mish, and K. Pierson, "Peridynamic Simulation of Damage Evolution for Structural Health Monitoring," *Vol. 8 Mech. Solids, Struct. Fluids*, p. 1, 2012.

[8] S. A. Silling and R. B. Lehoucq, "Convergence of peridynamics to classical elasticity theory," *J. Elast.*, vol. 93, no. 1, pp. 13–37, 2008.

[9] E. Madenci and E. Oterkus, *Peridynamic Theory and Its Applications*. New York, NY: Springer New York, 2014.

[10] S. A. Silling and R. B. Lehoucq, "Peridynamic theory of solid mechanics. Advances in Applied Mechanics," *Adv. Appl. Mech.*, vol. 44, pp. 73–168, 2010.

[11] F. Bobaru, J. T. Foster, P. H. Geubelle, and S. A. Silling, *Handbook of Peridynamic Modeling*. CRC Press, 2016.

[12] L. Meirovitch, *Fundamentals of Vibrations*, vol. 54, no. 6. 2001.

[13] Z. Bai, J. Demmel, J. Dongarra, A. Ruhe, and H. Vorst, "Templates for the Solution of Sparse Eigenvalue Problems," *Philadelphia SIAM*, 2000.

[14] M. L. Parks, D. J. Littlewood, J. a Mitchell, and S. a Silling, "Peridigm Users ' Guide," 2012.

[15] R. Grimes, J. Lewis, and H. Simon, "A shifted block Lanczos algorithm for solving sparse

symmetric generalized eigenproblems," *SIAM J. Matrix Anal. Appl.*, vol. 15, no. 1, pp. 228–272, 1994.
[16] R. B. Lehoucq, D. C. Sorensen, and C. Yang, *ARPACK Users' Guide*, no. 0. Society for Industrial and Applied Mathematics, 1998.
[17] S. A. Silling and E. Askari, "A meshfree method based on the peridynamic model of solid mechanics," *Comput. Struct.*, vol. 83, no. 17–18, pp. 1526–1535, 2005.
[18] J. Mitchell, S. Silling, and D. Littlewood, "A position-aware linear solid constitutive model for peridynamics," *J. Mech. Mater. Struct.*, vol. 10, no. 5, pp. 539–557, Nov. 2015.